JOURNAL OF PROPULSION AND POWER
Vol. 25, No. 6, November–December 2009

Thrust Measurement of a Multicycle Partially Filled Pulse Detonation Rocket Engine

Jiro Kasahara* and Masao Hirano†
University of Tsukuba, Tsukuba 305-8573, Japan
Akiko Matsuo‡ and Yu Daimon§
Keio University, Kanagawa 223-8522, Japan
and
Takuma Endo‡
Hiroshima University, Hiroshima 739-8527, Japan

DOI: 10.2514/1.42224

In the present research, we experimentally verified the partial-fill effect in a multicycle pulse detonation rocket engine. The intermittent thrust of a pulse detonation rocket engine was measured by using a spring-damper mechanism that smoothed this intermittent thrust in the time direction. The intermittent mass flow rates were assessed by gas cylinder pressure or mass difference measurement. The maximum specific impulse was 305 ± 9 s at an ethylene and oxygen propellant fill fraction of 0.130 ± 0.004. When the fill fraction was greater than 0.130, the specific impulse was increased as the partial-fill fraction was decreased. When the fill fraction was less than 0.130, the specific impulse was sharply decreased as the partial-fill fraction was decreased. This decrease was due to diffusion between propellant and purge gases and the short length of the transition from deflagration to detonation. The multicycle pulse detonation rocket engine had a partial-fill effect that may have been mainly due to the suctioned air and was consistent with the single-cycle partial-fill model of Endo et al. [Endo, T., Yatsufusa, T., Taki, S., Matsuo, A., Inaba, K., and Kasahara, J., "Homogeneous-Dilution Model of Partially-Fueled Simplified Pulse Detonation Engines," *Journal of Propulsion and Power*, Vol. 235, 2007, pp. 1033–1041.]

Nomenclature

A_e	=	control-volume surface area through which an exhaust jet flows
c	=	attenuation coefficient of a damper
F_f	=	force acting on the pulse detonation engine tube by the rail in the x direction
F_{kc}	=	force acting on the pulse detonation engine tube by the spring-damper system in the x direction
F_{lc}	=	force acting on the spring-damper system by the load cell in the x direction
F_p	=	force acting on the pulse detonation engine tube by the fluid in the x direction
F_t	=	force acting on the pulse detonation engine tube by the supplying tubes in the x direction
F_0	=	plateau thrust
$ff_{\mathrm{air,est}}$	=	estimated suctioned air fill fraction
$ff_{\mathrm{propellant}}$	=	propellant fill fraction
ff_{purge}	=	purge gas fill fraction
g	=	gravitational acceleration
I	=	impulse acting on the pulse detonation engine tube by the fluid in the x direction
I_{sp}	=	specific impulse
I_{total}	=	absolute value of the total impulse acting on the pulse detonation engine tube by the fluid in the $-x$ direction during all cycles
$I_{\mathrm{total},x}$	=	total impulse acting on the pulse detonation engine tube by the fluid in the $-x$ direction during all cycles
k	=	spring constant
M_c	=	molecular weight in the cylinder
m_d	=	mass of weight
$m_{\mathrm{propellant}}$	=	propellant mass during all of the cycles
m_{purge}	=	purge gas mass during all of the cycles
m_t	=	pulse detonation engine tube mass
p_a	=	ambient pressure around the control volume
p_e	=	exhausted-jet pressure on the control surface
R_c	=	gas constant of the gas in the cylinder
T_c	=	gas temperature in the cylinder
t	=	time
t_{cyc}	=	period of one cycle
t_{pl}	=	time during which the plateau thrust is maintained
t_{total}	=	time during all of the cycles
u_e	=	fluid velocity component in the x direction, on the control surface
u_x	=	fluid velocity component in the x direction
V	=	volume
V_c	=	volume of the cylinder
v_s	=	horizontal velocity of a solid element
v_w	=	velocity of the weight
x	=	horizontal axis fixed in the control volume
x_p	=	pulse detonation engine tube position in the x axis, of which the origin is the natural length of the point of a spring
Y	=	mass fraction that equals the propellant mass divided by the total mass of both the propellant and the purge gases
Δm_c	=	mass difference between the initial and final masses of the gas in the cylinder
Δp_c	=	pressure difference between the initial and final pressures of the gas in the cylinder

Received 16 November 2008; revision received 17 August 2009; accepted for publication 18 August 2009.

*Associate Professor, Department of Engineering Mechanics and Energy. Senior Member AIAA.
†Graduate Student, Department of Engineering Mechanics and Energy.
‡Professor, Department of Mechanical Engineering. Member AIAA.
§Graduate Student, Department of Mechanical Engineering. Member AIAA.

η = equivalence ratio
ρ_g = density of the gas
ρ_s = density of the solid

Subscripts

cs = control surface
cv = control volume

I. Introduction

A PULSE detonation engine (PDE) obtains thrust by generating detonation waves intermittently [1,2]. PDE review papers have been published by Kailasanath [3,4], Bazhenova and Golub [5], and Roy et al. [6]. The PDE for aerospace propulsion obtains thrust by blowing the detonated high-pressure gas down. The typical shape of a PDE is a straight tube, one end of which is closed while the other is open. After the tube is filled with propellant gas, the gas is ignited at the closed end of the tube and the detonation is initiated. A self-sustained detonation wave (which compresses the propellant by shock waves) propagates toward the open end of the tube, and the engine can be operated even if there are no compression mechanisms (such as compressors or pistons). Sufficient specific impulse (200–350 s) can be obtained even with the same fill pressure as that of ambient air (Zitoun and Desbordes [7], Morris [8], Endo and Fujiwara [9], Endo et al. [10], Wintenberger et al. [11], and Cooper et al. [12]), and thus a rocket engine with an extremely low combustor fill pressure [pulse detonation rocket engine (PDRE)] becomes possible [8]. The flow, as in a simplified PDE [9,10], can be achieved in the combustor of a PDRE because there is no interaction with the airbreathing mechanism (intake and compressor) installed before the combustor. The airbreathing PDE has been studied by many researchers, including Talley and Coy [13], Wintenberger and Shepherd [14], Harris et al. [15], Ma et al. [16], and Kojima and Kobayashi [17]. Moreover, it is easy to increase the specific impulse by using a mechanism (an extension tube for partial filling [18], an ejector [19,20], or a nozzle [8]) installed after the combustor. In the PDRE, the specific impulse can be increased by partially filling the detonation tube with propellant. With a partial fill, the burned gas generated during the previous cycle remains in the tube and purge gas is added in front of this propellant in the detonation tube. The burned gas and purge gas are called the inertia gas in this paper. As the detonation wave propagates in the propellant gas with which the detonation tube is partially filled, the burned high-pressure gas is expanded and accelerated toward the open end of the tube. Because the burned gas pressure force acts on the inertia gas, the burned gas obtains reaction force from the inertia gas. The closed-end thrust wall of the detonation tube obtains a larger specific impulse in the partially filled tube than it would obtain in a fully filled one. The specific impulse generally increases with the decrease of the fill fraction. By this increase of specific impulse in the partially filled tube, the intermittent thrust engine, like a PDE, is distinguished from other aerospace steady-state flow engines. In the PDE system, an ambient air inertia can be available for increasing thrust by using a simple straight tube without a ducted fan. Many experimental, computational, and analytical works have been performed to examine the effects of partial filling on single-tube and single-cycle PDEs. Endo and Fujiwara [9] analyzed the performance of the straight-tube PDE fully filled with propellant, and formulated the pressure history at the thrust wall of the closed end of the PDE tube with no empirical parameters. In a subsequent study, Endo et al. [10] formulated more accurately the pressure decay portion of this thrust-wall pressure history.

Recently, Endo et al. [21] proposed a single-cycle partially filled PDE performance model based on the experimental results of Zhdan et al. [22], showing that the impulse generated in the PDE tube during one cycle operation did not depend on the detonation initiation points. Endo et al. assumed that the thrust of the partially filled PDE tube was identical to the thrust of the fully filled PDE tube with propellant gas homogeneously mixed with inertia gas. Their model [22] was in good agreement with the results of the experiments and the computational fluid dynamics (CFD) calculations to within 15%. Sato et al. [18] obtained the specific impulse of a partially filled PDE tube with a hydrogen–oxygen mixture by using CFD, and they proposed the following semi-empirical formula for the specific impulse:

$$\frac{I_{\mathrm{sp}}}{I_{\mathrm{sp}}|_{ff=1}} = \frac{1}{\sqrt{Y}}$$

This equation allows one to definitely account for the effect of partial filling. Specifically, the specific impulse was in inverse proportion to the square root of the ratio of the mass of the propellant to the mass of all gas. As a result, the thrust also increases. This empirical equation gives the same results as those of the model of Endo et al. [21] in almost all of the fill fraction ($\phi \geq 0.01$). Although the specific impulse increases infinitely as the fill fraction approaches zero, such a phenomenon never occurs physically. Accordingly, this equation cannot be applied if the fill fraction is extremely small.

In a recent study, Kasahara et al. [23] showed the specific impulse upper limit in the small fill fraction region by using a partially filled shock tube with an open-ended extension tube. In their experiment, high-pressure inert gas in the shock tube expanded instantaneously into the ambient inertia air in the extension tube. This specific impulse upper limit could be theoretically explained by the bubble model (Cooper [24] and Cooper et al. [25]). Kasahara et al. [23] showed that the partial-fill effect is essentially related to the interaction between the pressure wave (shock and expansion waves) propagated in the gas and the contact discontinuity surface. Although the single-cycle PDE gas dynamics in a partially filled tube had been well clarified, the multicycle PDE gas dynamics in a partially filled tube had not been sufficiently verified, because the inertia gas in the multicycle PDE operation was not only an inert gas but also a burned gas generated during a previous cycle, and the negative gauge pressure in the exhaust phase could cause the suction of ambient air at the open end of the tube.

Schauer et al. [26] reported that a multicycle PDE had its specific impulse increase when the fill fraction decreased. Cooper et al. [25] compared their single-cycle model with the multicycle data of Schauer et al. [26] by assuming that multicycle operation was equivalent to a series of ideal single cycles. Schauer et al. [26] did accurate measurements of thrust, fill fraction, and specific impulse in the multicycle PDEs, but they only described the thrust and mass flow rate measurement setup briefly in their paper, and they did not discuss the fraction between the burned gas and the purge gas (air) in the tube. In this experimental study, we introduced a spring-damper mechanism that smoothed the impulsive thrust generated by the multicycle PDE operation. We showed that this mechanism was effective for obtaining smooth thrust from a single-tube PDE. In the present study, we achieved multicycle PDE tube operation while varying the fill fraction, and we verified the increase in specific impulse by comparing the present experimental results with the partial-fill model of Endo et al. [21], which took into account the purge gas, the previous-cycle burned gas, and the suctioned air.

II. Experimental Equipment and Thrust Measurements

We used ethylene–oxygen mixtures as propellant. These mixtures have very high detonability and have been used in a number of experimental works [27–31] due to reliable detonation initiations in each cycle in the multicycle PDE operation. In the present experiment, the impulsive thrust in the multicycle PDE operation was approximately 8000 N, lasting 10 ms in each cycle. Such an impulsive thrust could not be directly measured based on the typical load cells because of the measurement limits of force and time resolution. The spring-damper mechanism of our device was placed between the load cell and the impulsive-thrust-wall of the PDE tube. This mechanism could smooth the impulsive thrust in the direction of time. Mechanical model calculation was performed to set an appropriate spring constant and damping coefficient. The propellant mass flow of the PDE was intermittent due to its propellant supply system

typically having high-frequency valves. In the present experiment, we employed the measurement method of one-cycle mass flow, which was obtained from the directly weighted total mass decrease in the propellant cylinders divided by the total cycle number (total mass-weighted method). The other method we employed was to measure the cylinder pressure differences before and after experiments and calculate mass differences from these pressure differences and the equation of state. However, the latter method was calibrated by the former total mass-weighted method, in which a 1 liter gas cylinder and electrobalance were used.

A. Experimental Devices

A schematic of the experimental apparatus is shown in Fig. 1, and Fig. 2 is a photograph of the experimental devices. The four ball-bearing wheels of the PDE tube (a cylindrical tube connected to a tapered tube) are attached to two parallel guide rails. The thrust generated at the tapered closed end of the PDE tube is measured by the load cell through the spring-damper mechanism. The PDE tube can slide on the rail before and after detonation in the x direction with little friction. The propellant gases are supplied to the PDE tube through the top portion of the tapered closed-end tube. The ethylene and oxygen gases as propellant are mixed at and supplied through the cross joint, directly connecting to the tapered closed-end tube. The helium gas as a purge gas is also supplied to the PDE tube through the cross joint. This cross joint is attached to the three tubes with solenoid valves, as shown in Fig. 1. The valve mass flow rate and operation

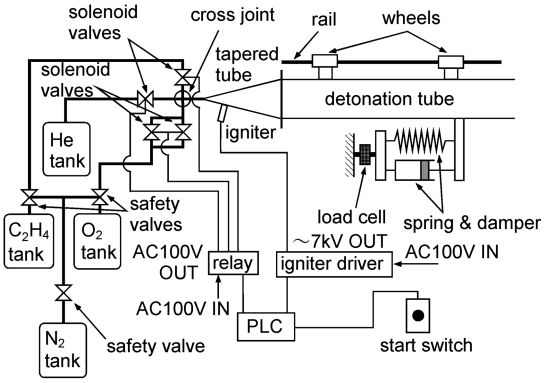

Fig. 1 Schematic diagram of the experimental device.

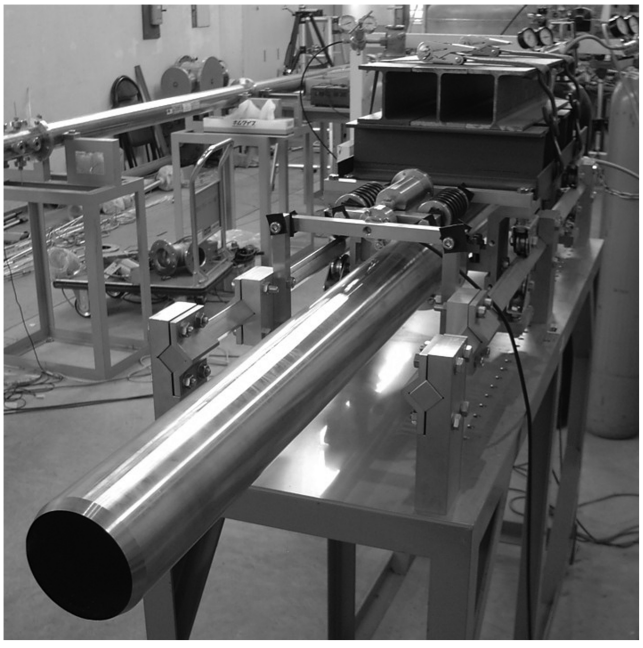

Fig. 2 Photograph of the experimental device.

frequency are managed by a programmable controller. One solenoid valve is used for ethylene gas and one is used for helium gas. Two parallel solenoid valves are used for oxygen gas (Figs. 1 and 3). These solenoid valves are connected to the propellant and purge gas cylinders through flexible tubes. The igniter is supplied with power by the igniter controller and is controlled by a programmable controller with a 1 ms time resolution sequence. The igniter is an automobile spark plug (Bosch, FR8DPIX). The voltage in the electrode gap of the spark plug is approximately 7 kV. This spark plug gap voltage can be monitored during the PDE operation. The length of the cylindrical tube is 2000 mm, and the inner diameter of the cylindrical tube is 100 mm. The material of the tube is Japanese industrial standard stainless steel (JIS SUS) 316. The open end of the PDE tube is exposed to the ambient air. The solenoid valves attached to the tapered tubes are shown in Fig. 3. The tapered tube has a half-opened angle of 15 deg and a volume of 0.47 liters. If a cylindrical tube is replaced by a tapered tube with the same cross-sectional area, the tapered tube length is 60 mm. If the PDE tube is replaced by a 100 mm constant-inner-diameter cylindrical tube, the reduced total length of this cylindrical tube is 2060 mm. The ignition point is on the inside of the tapered tube. Although the tapered tube has six ports for igniters, we use only one port that is 157 mm from the open end of the tapered tube (2159 mm from the open end of the PDE tube), as shown in Fig. 3. The tapered tube is preheated to 100°C or hotter. The solenoid valves are directly driven two-port valves (CKD Corporation., AB-41-02-1, normally closed), as shown in Fig. 3. The orifice diameter, the value of the coefficient of the valve (Cv value), and the maximum primary pressure of the solenoid valve are 1.5 mm, 0.1, and 5 MPa, respectively.

B. Experimental Conditions

Figure 4 shows the operation sequence when the operation cycle is 200 ms. When the propellant (ethylene and oxygen) valves are opened, the purge gas (helium) valve is closed and vice versa. The plug igniter is sparked just after the control signal falls below a trigger level. Figure 4 shows sequence A, in which the time during which the propellant is supplied is identical to the time for purging by helium gas. Stable multicycle operation is achieved when the operation frequency is comparatively low. At such a low frequency, the volume filled with propellant or purge gas is large, and therefore the length identical to the purge gas volume, divided by the PDE tube cross-sectional area, becomes large as well [31,32]. If the operation frequency increases over these criteria, the purging becomes insufficient due to decreased helium purging time. With this type of high-frequency operation, a stable multicycle operation cannot be achieved due to improperly timed ignition caused by diffusing and mixing of the previous-cycle high-temperature burned gas with the unburned gas. To prevent this improperly timed ignition, when the time for supplying propellant is below 60 ms, we employ sequence B (Fig. 5), in which the time for supplying propellant is half as long as for purging. By using sequence B, multicycle operations can be performed in the conditions of higher frequency and lower fill

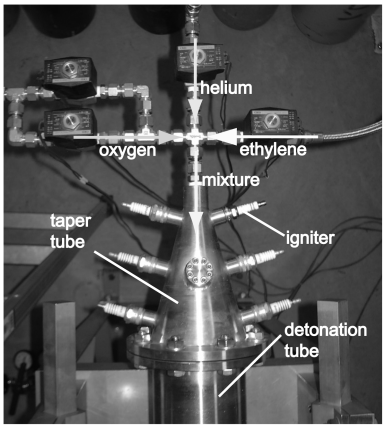

Fig. 3 Tapered tube and solenoid valves.

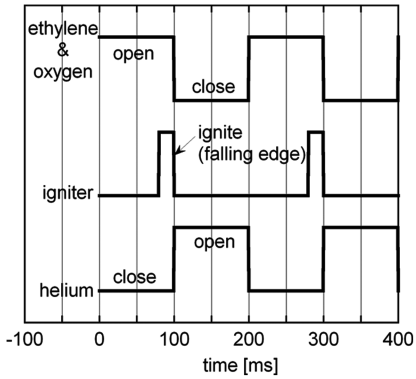

Fig. 4 Sequence A (mixture:helium = 1:1).

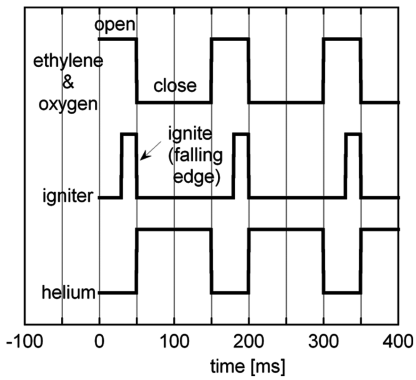

Fig. 5 Sequence B (mixture:helium = 1:2).

fraction. In the present experiment, the total operation time of one cycle's time multiplied by the cycle number does not exceed 3000 ms. The experimental conditions are shown in Table 1. The primary pressure of all the valves is 3 MPa. The time for supplying is varied from 200 to 40 ms, in 11 steps. The multicycle operation is performed in sequence A with shots 1–7, and in sequence B with shots 8–11.

C. Thrust Measurements

In the present study, we use the load cell (Aikoh Engineering, DUD-100K) to measure the thrust during multicycle operation. The maximum load of this load cell is ±1000 N. The oscilloscope receives and records input from this load cell through an amplifier (Unipulse, F304A). The mechanical model for measuring the thrust generated by the PDE tube is shown in Fig. 6. The control volume is defined by the broken line shown in Fig. 6. The motion of the PDE tube in the x direction is derived using the following equation:

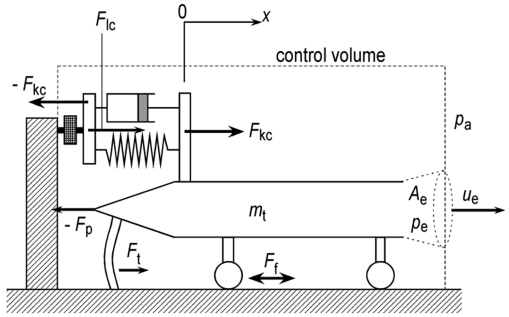

Fig. 6 Model for thrust measurement.

$$F_p + F_{kc} + F_f + F_t = m_t \ddot{x} \tag{1}$$

The motion of the load cell in the x direction is determined using the following equation:

$$-F_{\mathrm{lc}} + F_{kc} = 0 \tag{2}$$

The motion of the total control volume in the x direction can be shown by

$$F_{\mathrm{lc}} + F_f + F_t + A_e p_a - A_e p_e = \int_{\mathrm{cs}} \rho u_x (\boldsymbol{u} \cdot \boldsymbol{n})\, \mathrm{d}A + \frac{\mathrm{d}}{\mathrm{d}t} \int_{\mathrm{cv}} \rho u_x \, \mathrm{d}V + \frac{\mathrm{d}}{\mathrm{d}t} \int_{\mathrm{cv}} \rho_s v_s \, \mathrm{d}V \tag{3}$$

The total impulse of the PDE tube is calculated as follows:

$$I_{\mathrm{total},x} = \int_0^{t_{\mathrm{total}}} F_p \, \mathrm{d}t \tag{4}$$

From Eqs. (1), (2), and (4), we can obtain the following equation:

$$I_{\mathrm{total},x} = -\int_0^{t_{\mathrm{total}}} (F_{\mathrm{lc}} + F_f + F_t)\, \mathrm{d}t + m_t \int_0^{t_{\mathrm{total}}} \frac{\mathrm{d}v}{\mathrm{d}t}\, \mathrm{d}t$$

in which the condition of

$$\int_0^{t_{\mathrm{total}}} \frac{\mathrm{d}v}{\mathrm{d}t}\, \mathrm{d}t = 0$$

is satisfied due to the initial and final PDE tube velocities being zero. Therefore, we obtain

$$I_{\mathrm{total},x} = -\int_0^{t_{\mathrm{total}}} (F_{\mathrm{lc}} + F_f + F_t)\, \mathrm{d}t \tag{5}$$

Because the right-moving direction in Fig. 6 is positive in the x direction, the value of $I_{\mathrm{total},x}$ is usually negative. In Eq. (5), the force generated by the supplying tube F_t is neglected due to its magnitude being assumed to be smaller than those of other forces. The PDE tube can slide on the rail in the positive or negative direction of x with little

Table 1 Experimental conditions

Shot number	Supplying pressure, MPa	Fueling duration, ms	Purging duration, ms	Frequency, Hz	Operating duration, ms	Propellant fill fraction, -
1	3	200	200	2.5	2800	0.264
2	3	175	175	2.9	2800	0.252
3	3	150	150	3.3	3000	0.223
4	3	125	125	4.0	3000	0.203
5	3	100	100	5.0	3000	0.155
6	3	85	85	5.9	2890	0.130
7	3	70	70	7.1	2940	0.117
8	3	60	120	5.6	2880	0.106
9	3	50	100	6.7	3000	0.087
10	3	45	90	7.4	2970	0.083
11	3	40	80	8.3	3000	0.075

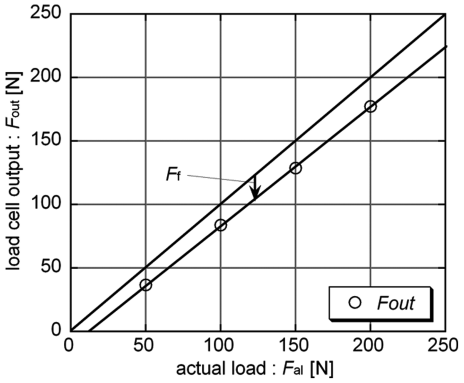

Fig. 7 Measurement of static friction.

friction on the bearings, wheels, or rails. We obtain this static friction force by measuring the difference between the load on the PDE tube in the x direction by the calibrated weight and the load cell output. This result is shown in Fig. 7. From this figure, we find the static friction is approximately 20 N in the load range from 0 to 200 N. We also verified the high linearity of the load cell. In the multicycle PDE operation, the dynamic friction force of the rails and bearings exists, but this force is less than the force of the static friction, and its vector periodically varies in the positive and negative directions of x. Because the temporally averaged dynamic force is much less than the other forces, we neglect the dynamic friction force F_f. We finally obtain the following expression regarding total impulse:

$$I_{\text{total},x} = -\int_0^{t_{\text{total}}} F_{\text{lc}}\,\mathrm{d}t \tag{6}$$

We use Eq. (6) to obtain the temporally integrated impulse acting on the PDE tube $I_{\text{total},x}$.

D. Smoothing of Pulsed Thrust by Using the Spring-Damper Mechanism

As the plateau pressure near the thrust wall of the PDE tube is maintained at approximately 1 MPa for a few milliseconds, the impulsive thrust on the wall is approximately 8000 N. As shown in Fig. 8, this impulsive thrust on the PDE tube is smoothed by the damping system. In this experiment, the additional H-beam weight of 45 kg is attached to the PDE tube. The total mass of the PDE tube m_t, including this additional mass, is 100 kg. To design this mechanism, we had to determine two characteristic parameters: the viscous damping coefficient c and the spring constant k. To do so, we calculated the impulsive force history on the load cell using the following model. The impulsive thrust of the PDE tube is approximately rectangular, as shown and defined in Fig. 9, which can be expanded to a Fourier series, as shown in the following equations. This rectangular thrust is defined by the operation cyclet_{cyc}, plateau thrust F_0, and time for maintaining the plateau thrust t_{pl}. The position of the multicycled PDE tube $x_p(t)$ can be expressed in the following form:

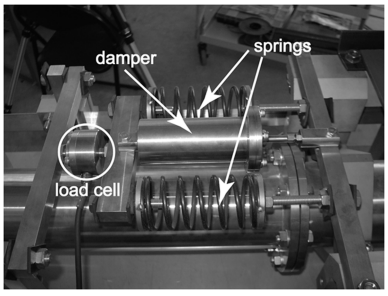

Fig. 8 Damping system.

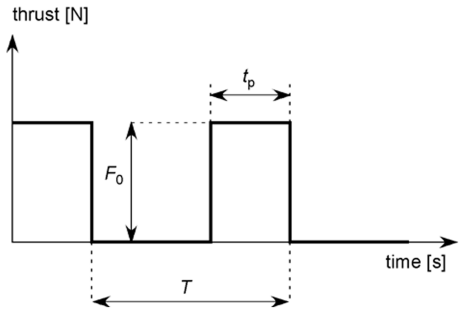

Fig. 9 Pulse wave for simulation.

$$x_p(t) = a_0 + \frac{1}{\pi}\sum_{n=1}^{\infty}(a(n)\cos(n\omega t - \phi(n)) + b(n)\sin(n\omega t - \phi(n)));$$

$$a(n) = \frac{\omega_n^2}{\sqrt{(\omega_n^2 - n^2\omega^2) + (2\xi\omega_n\omega n)^2}}\delta_{\text{st}}\frac{\sin(n\alpha)}{n};$$

$$b(n) = \frac{\omega_n^2}{\sqrt{(\omega_n^2 - n^2\omega^2) + (2\xi\omega_n\omega n)^2}}\delta_{\text{st}}\frac{1-\cos(n\alpha)}{n}$$

where

$$\alpha = \frac{2\pi t_{\text{pl}}}{t_{\text{cyc}}}; \qquad \omega = \frac{2\pi}{t_{\text{cyc}}}; \qquad \delta_{\text{st}} = \frac{F_0}{k}; \qquad \omega_n = \sqrt{\frac{k}{m_p}};$$

$$\xi = \frac{c}{2\sqrt{km_p}}; \qquad a_0 = \delta_{\text{st}}\frac{\alpha}{2\pi}; \qquad \phi(n) = \operatorname{atan}\left[\frac{2\xi[\mathrm{n}(\omega/\omega_{\mathrm{n}})]}{1-[\mathrm{n}(\omega/\omega_{\mathrm{n}})^2}\right]$$

By using this PDE–tube position $x_p(t)$, the thrust on the load cell, $-F_{\text{lc}} = -F_{kc} = c\dot{x}_p + kx_p$, can be obtained from Eq. (2). To determine the design parameters, t_{cyc} is set at 170 ms as a typical experimental condition, in which sequence A is employed and the propellant and purging times are 85 ms. The plateau thrust F_0 is set at 7850 N due to the following calculation, in which the inner radius of the cylindrical PDE tube is 50 mm and the plateau pressure is 1 MPa:

$$F_0 = 0.05 \times 0.05 \times 3.14 \times 10^6 = 7850 \text{ [N]}$$

The plateau pressure time is set as $t_p = 1$ [ms] according to the condition in which the typical total impulse of the PDE tube is identical to $t_p F_0$. The PDE tube mass and the spring constant are given as $m_t = 100$ [kg] and $k = 10,000$ [N/m] $\times 2 = 20,000$ [N/m], respectively. The transient and damped oscillations of this system are calculated by using the second-order differential equation $\ddot{x}_p = -\frac{c}{m_t}\dot{x}_p - \frac{k}{m_t}x_p$. We obtain the solutions of the piston position x_p, of which the typical case is plotted in Figs. 10 and 11. In these calculations, the initial velocity of the PDE tube is zero, and the initial position is the maximum displacement position in the multicycle operation. This system is also required to shorten the transient oscillation time. In the present experiment, the total operation time of the multicycle operation is 3 s. We employ the damper attenua-

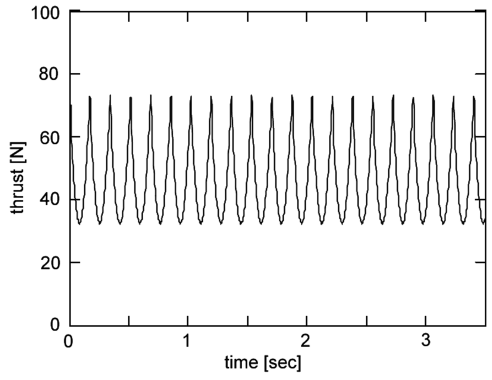

Fig. 10 Thrust history ($c = 250$ Ns/m).

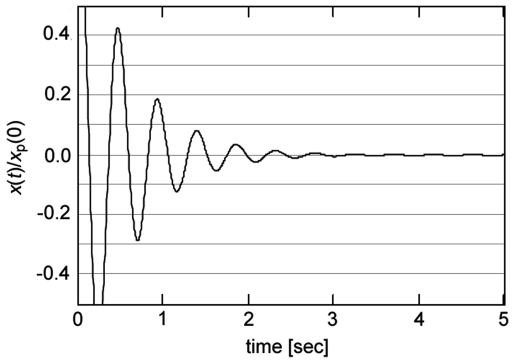

Fig. 11 Damping oscillation ($c = 250$ Ns/m).

tion coefficient, which enables the initial amplitude to decrease to 10% of its initial value within 1.5 s. From the calculations, we find that this condition is satisfied when $c \geq 250$ Ns/m. Therefore, the experimental conditions are $c = 250$ Ns/m and $k = 20,000$ N/m. Figures 10 and 11 show the cyclic and transient oscillations in this condition. The damper used in this experiment is shown in Fig. 12. We created this damper for this experiment, so that we could modify the orifice of the piston and the fluid in the cylinder. The damper has two orifices, 3.5 and 5.5 mm in diameter, as shown in Fig. 12. The working fluid is automobile oil [SAE (Society of Automotive Engineers) viscosity 5W-30, 3.8 mm^2/s and more). The attenuation coefficient of the damper is determined by the following preliminary experiment. The axis of the damper is set vertically, and the piston is below the cylinder part. A weight with a mass of 0.7134 kg is suspended from the piston of the damper and descends. The descent velocity of the weight is measured using a video camera. Because the derivation of the descent velocity is negligible, the attenuation coefficient of the damper can be determined by the equation $c = m_d g / v_w$. The attenuation coefficient of the damper, depending on the piston position, is shown in Fig. 13. The initial position of the piston is zero on the horizontal axis of Fig. 13, when the piston is attached to the bottom of the cylinder and the total

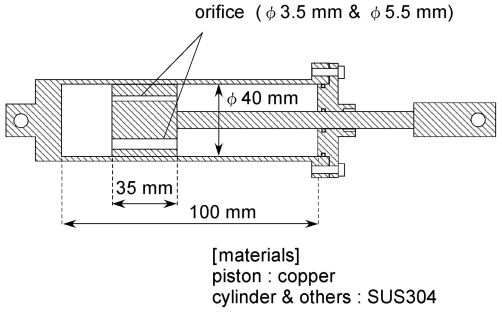

Fig. 12 Cross-sectional diagram of damper.

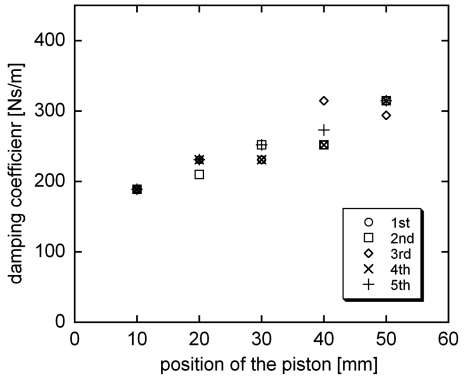

Fig. 13 Damping coefficient versus position of piston.

length of the damper is at its shortest. Figure 13 shows that the attenuation coefficient increases as the piston position increases. The designed attenuation coefficient of 250 Ns/m is satisfied at the piston position of 30 mm. Thus, to realize simulated damping, the total damper length is adjusted to the length at which the piston oscillates, around 30 mm all the time.

E. Measurements of the Mass Flow Rate of Propellant and the Filling Rate

To obtain specific impulses of the PDE tube, we had to properly measure the mass flow rates of the propellant. In the present study, the mass flow rates of the propellant are measured using two methods. In the first method, the mass flow rate is obtained by measuring the pressure difference between the before and after operations. If, in the constant-volume cylinders, the gas temperatures are constant, we obtain

$$\Delta m_c = \Delta p_c \frac{M_c V_c}{R T_c} \tag{7}$$

Therefore, if we obtain Δp_c, then Δm_c and the mass flow rate can be calculated. In the present experiment, the mass flow rate of the ethylene supply system is calibrated using oxygen for safety reasons. We assume that the molar flow ratio of ethylene is equivalent to that of oxygen in this system.

The mass flow rate can also be obtained by the direct measurement of cylinder mass differences before and after operations using an electrobalance. In this method, the mass flow rate data can be obtained in each experimental shot. If we employ this method, we cannot neglect the mass of the gas remaining in the flexible tubes connected between the cylinders and the electromagnetic valves. As shown in Fig. 14, the two stop valves are attached to the separation part between a regulator and a tube. These two valves minimize the mass loss in this separation before the cylinder weight measurement by the balance. Figure 15 shows measurement results of both methods, which are almost equal to one another. We noted that the

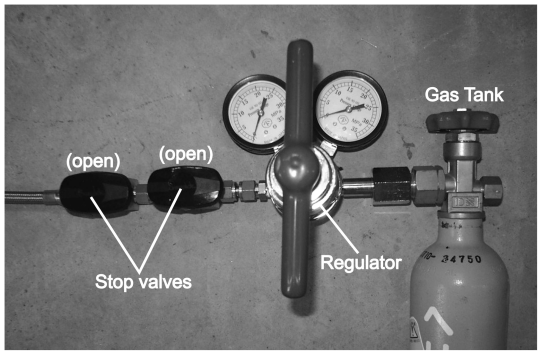

Fig. 14 Stop valves (connected).

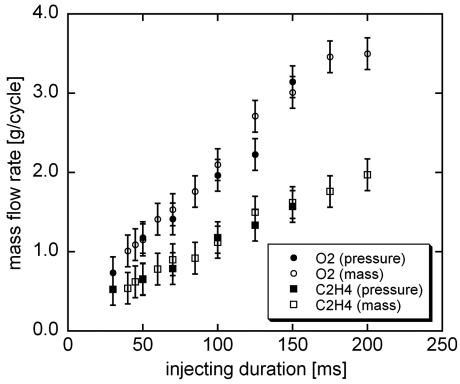

Fig. 15 Comparison of mass flow rates between pressure and mass measurements.

ethylene mass flow rate determined by the pressure difference method, in which the oxygen molar flow rate is assumed to be equivalent to that of ethylene, is identical to that determined by the mass difference method.

In the following description, the results of the mass flow rate determined by the mass difference method will be used. The propellant fill fraction of the PDE tube is calculated by using the measured mass flow rate. The volumes of the tapered tube and the cylindrical tube are 0.47 and 15.71 liters, respectively. The PDE tube, which is the sum of the tapered and cylindrical tubes, has a volume of 16.18 liters. The propellant fill fraction in each cycle is calculated by the following procedure. The temperature and pressure in the PDE tube are assumed to be 290 K and 1 atm, respectively. The volume flow rate can be obtained from the mass flow rate and the equation of state of each gas. The fill fraction can be obtained from the total volumes of ethylene and oxygen in one cycle divided by the PDE tube volume. This fill fraction is plotted against the time for supplying propellant shown in Fig. 16.

III. Results and Discussion

A. Thrust and Impulse

The typical thrust history measured by the load cell is shown in Fig. 17. The load cell data are recorded after processing by the low-pass filter (below 60 Hz) to reduce the electrical noises caused by the power source. In every shot, the thrust in the first cycle is larger than that in the second and later cycles. We considered this to be due to the effect of the high-density gases remaining in the flexible tubes before the start of the operation. Before the first cycle only, these tubes are filled with high-pressure gases just before the electromagnetic valves are activated. Therefore, the gases are injected at higher pressure and fill the PDE tube at a larger volume in the first cycle than in the second and later cycles. The total impulse in multicycle operation can be defined as follows:

$$I_{\text{total}} = |I_{\text{total},x}| = \left| -\int_0^{t_{\text{total}}} F_{\text{lc}}\, \mathrm{d}t \right| \tag{8}$$

The impulse per cycle can be obtained using the following equation:

$$I_{\text{cyc}} = \frac{I_{\text{total}}}{N_{\text{cyc}}} \tag{9}$$

The impulse per cycle I_{cyc} for each cycle is plotted against the time for supplying propellant in Fig. 18. In this figure, we see that I_{cyc} decreases abruptly as the time for supplying propellant decreases to 50 ms or less. As mentioned previously, when the time for supplying propellant is below 60 ms, sequence B is employed to stabilize the PDE operation. Figure 19 (shot 11) shows the typical thrust history in such a sequence B. An approximately 1 Hz small-amplitude oscillation is superimposed on the oscillated thrust history. As Fig. 19 shows, in sequence B, the multicycle operation is not considered to be perfectly stabilized. These oscillation phenomena probably occur because, as the propellant volume becomes much smaller than the purge gas and/or previous-cycle combusted gas, the propellant density and length become smaller and shorter by diffusion, respectively, and they are not sufficient to initiate a detonation wave in the PDE tube. By the additional measurement (using a shadowgraph optical system and a high-speed video camera), we confirm that in the premixed stoichiometric ethylene–oxygen 0.7 atm and 290 K mixture in the square cross-sectional smooth-wall tube without an obstacle, the detonation initiation length is larger than the square tube height (50 mm). Assuming this detonation-initiation-length requirement in the PDE tube, shown in Fig. 1, the condition $ff > 0.05$ is necessary for detonation initiation, and this condition is consistent with the result of Fig. 19 (shot no. 11, $ff = 0.075$). Specific impulses can be calculated from the measured total impulse and the measured total mass (C_2H_4-O_2-He) using the following equation:

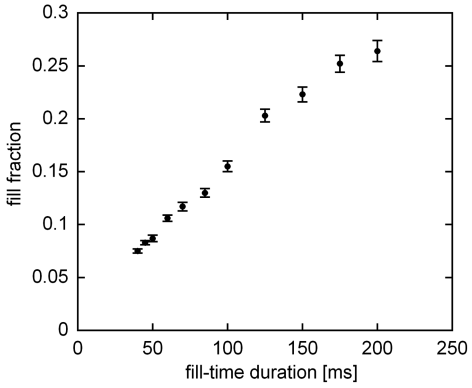

Fig. 16 Fill fraction of mixture versus fueling duration.

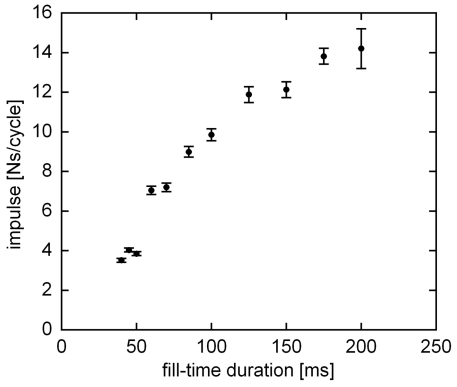

Fig. 18 Impulse versus fueling duration.

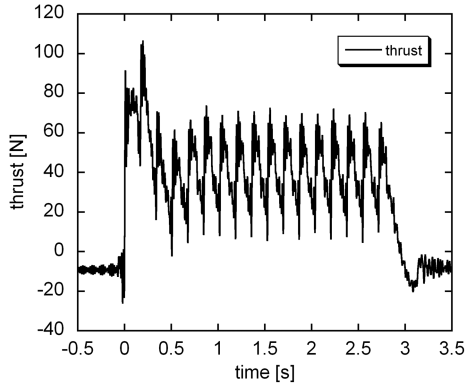

Fig. 17 Thrust history of 85 ms fueling and 85 ms purging operation (shot no. 6, 5.9 Hz).

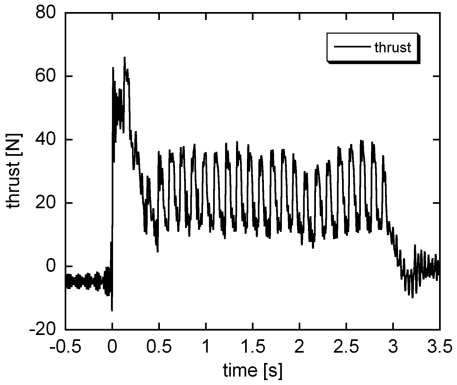

Fig. 19 Thrust history of 40 ms fueling and 80 ms purging operation (shot no. 11, 8.3 Hz).

Table 2 Experimental results

Shot number	Number. of cycles N	Impulse I_{all}, Ns	Impulse per cycle I_{all}/N, Ns/cycle	Propellant mass flow per cycle $m_{propellant}/N$, g/cycle	Helium mass flow per cycle m_{purge}/N, g/cycle	Total mass flow per cycle $(m_{propellant} + m_{purge})/N$, g/cycle	Equivalence ratio η, -	Volume of propellant at 290 K and 1 atm V, L/cycle	Fill fraction ff, -	Specific impulse I_{sp}, s
1	7	99 ± 4	14 ± 1	5.5 ± 0.2	0.657 ± 0.02	6.2 ± 0.2	1.93	4.3 ± 0.2	0.26 ± 0.01	240 ± 10
2	8	111 ± 4	13.8 ± 0.4	5.22 ± 0.16	0.700 ± 0.02	5.92 ± 0.16	1.75	4.07 ± 0.12	0.252 ± 0.008	238 ± 7
3	10	121 ± 4	12.1 ± 0.4	4.63 ± 0.14	0.540 ± 0.02	5.17 ± 0.14	1.85	3.61 ± 0.11	0.223 ± 0.007	239 ± 7
4	12	143 ± 5	11.9 ± 0.4	4.21 ± 0.13	0.625 ± 0.02	4.83 ± 0.13	1.90	3.29 ± 0.10	0.203 ± 0.006	251 ± 8
5	15	148 ± 5	9.85 ± 0.30	3.22 ± 0.10	0.407 ± 0.01	3.63 ± 0.10	1.83	2.51 ± 0.08	0.155 ± 0.005	277 ± 8
6	17	153 ± 5	8.99 ± 0.27	2.69 ± 0.08	0.312 ± 0.01	3.00 ± 0.08	1.79	2.10 ± 0.06	0.130 ± 0.004	305 ± 9
7	21	151 ± 5	7.20 ± 0.22	2.43 ± 0.07	0.305 ± 0.01	2.73 ± 0.07	2.02	1.90 ± 0.06	0.117 ± 0.004	269 ± 8
8	16	113 ± 4	7.04 ± 0.21	2.19 ± 0.07	0.425 ± 0.01	2.62 ± 0.07	1.90	1.71 ± 0.05	0.106 ± 0.003	274 ± 8
9	20	77 ± 3	3.9 ± 0.1	1.8 ± 0.1	0.500 ± 0.02	2.3 ± 0.1	1.94	1.4 ± 0.1	0.087 ± 0.003	170 ± 10
10	22	89 ± 3	4.0 ± 0.1	1.7 ± 0.1	0.368 ± 0.01	2.1 ± 0.1	1.97	1.3 ± 0.1	0.083 ± 0.002	200 ± 10
11	25	88 ± 3	3.5 ± 0.1	1.6 ± 0.1	0.320 ± 0.01	1.9 ± 0.1	1.84	1.2 ± 0.1	0.075 ± 0.002	190 ± 10

$$I_{sp} = \frac{I_{total}}{(m_{propellant} + m_{purge})g} \tag{10}$$

The specific impulse of every shot is listed in Table 2.

B. Specific Impulse

Figure 20 shows the specific impulses obtained from this multicycle experiment and from single-cycle calculation using the partial-fill model of Endo et al. [21], which are plotted against the propellant (C_2H_4-O_2) fill fraction at 1 atm and 290 K, $ff_{propellant}$, in the PDE tube. In the figure, the specific impulse increases as the partial-fill fraction decreases in the region $ff_{propellant} \geq 0.130$. From this figure, we can verify that the partial-fill effect exists in the multicycle operation. When the propellant fill fraction is 0.130 ± 0.004, the specific impulse achieves a maximum value of 305 ± 9 s. The specific impulse sharply decreases as the fill fraction decreases in the region $ff_{propellant} < 0.130$.

Both the partial-fill model of Endo et al. [21] and the bubble model of Cooper et al. [24,25], which can estimate the maximum specific impulse in the case of an extremely small fill fraction, operate under the assumption that the fuel and oxidizer are perfectly reacted. In these models, in most of the cases, specific impulses do not decrease as the fill fractions decrease to zero. The inert gas open-shock-tube experiment by Kasahara et al. [23] showed the specific impulse upper limit and no decrease as the fill fraction decreased in the small fill fraction region. Recently, Kasahara et al. [31] showed that for stable operation of a multicycle ethylene–oxygen propellant PDE, the sufficient purge gas thickness divided by the tube diameter ($L/D \geq 3.12$) was necessary. In the present experiment, in the region $ff_{propellant} < 0.087$, the nondimensional purge gas thickness L/D was 2.27 ($ff_{propellant} = 00.075$), 2.61 ($ff_{propellant} = 00.083$), and 3.55 ($ff_{propellant} = 0.087$), and it might not be sufficient for stable operation. From these analytical and experimental results, we conclude that this sharp decrease is due to diffusion between the fresh mixture and the helium purge gas and an imperfect transition from a deflagration to a detonation wave.

We next compare our experimental results with the partial-fill model calculation results of Endo et al. [21]. The specific impulses for the partial-fill model of Endo et al. are shown by open symbols in Fig. 20. Figure 21 is a schematic picture of the initial gas distribution in the PDE tube in the model of Endo et al. The filling gases are a

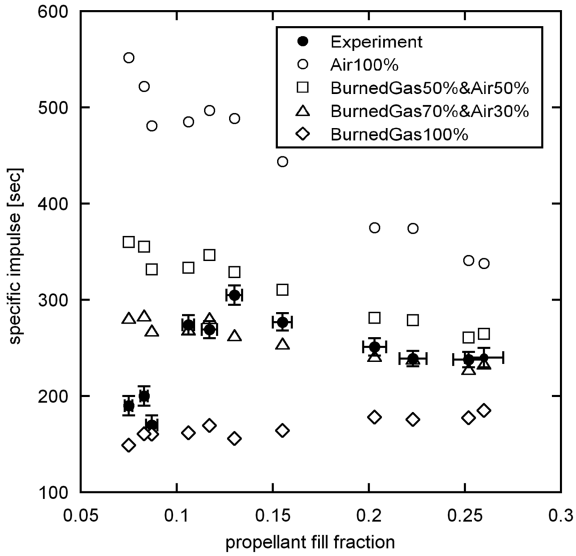

Fig. 20 Comparison of specific impulses between experimental results and the partial-fill model calculation of Endo et al. [21] The open symbols show model calculation results. Air100% or BurnedGas100% mean that the remaining gas is air only or burned gas only, respectively. BurnedGas50%&Air50% or BurnedGas70%&Air30% mean that 50 or 70% of the remaining gas is burned gas and the remaining gas is air, respectively.

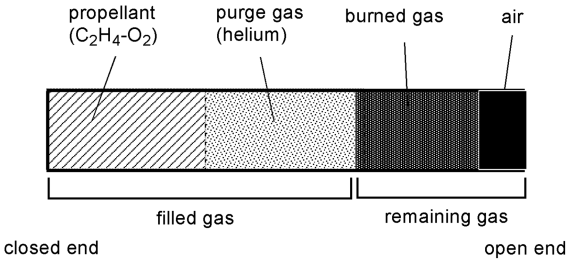

Fig. 21 Initial gas condition used in the partial-fill model of Endo et al. [21].

propellant and a purge gas, and the remaining gases are burned gas and air. The propellant is an ethylene–oxygen mixture at 1 atm and 290 K, and the equivalence ratio of the propellant mixture is used in Table 2. The purge gas is helium at 1 atm and 290 K. The burned gas is an isentropically expanded propellant (in the previous cycle) from the Chapman–Jouguet state to 1 atm with an equilibrium composition, which was obtained by the STANJAN chemical thermodynamics software [33]. The suction air, which is assumed to be suctioned from the space around the open end of the PDE tube, has a state of 1 atm and 290 K. The experimental specific impulses are between the calculated results of 50 and 70% remaining gas as burned gases when the partial-fill fraction was above 0.1 in Fig. 20. Therefore, assuming that Endo's single-cycle partial-fill calculation model can correctly predict the multicycle partially fueled PDE's specific impulse, we cannot assume that only burned gas remained inside the PDE tube. As the burned gas density is between 0.093 and 0.097 kg/m^3, which is much lower than that of the propellant (1.28 kg/m^3 at 1 atm and 300 K) or air (1.22 kg/m^3 at 1 atm and 300 K), the partial-fill effect by the burned gas inertia may be negligible. The partial-fill effect observed in the present experiment may be mainly due to the air existing near the open end of the PDE tube, which is suctioned by the negative gauge pressure during the exhaust phase of the PDE cycle.

Based on the following equation, we can estimate the fill fraction of the suctioned air to the PDE tube $ff_{\text{air,est}}$:

$$ff_{\text{air,est}} = (1 - ff_{\text{propellant}} - ff_{\text{purge}}) \times \left(0.5 - 0.2\frac{I_{\text{sp,BG50\%\&Air50\%}} - I_{\text{sp}}}{I_{\text{sp,BG50\%\&Air50\%}} - I_{\text{sp,BG70\%\&Air30\%}}}\right) \tag{11}$$

where ff_{purge} is the purge gas volume fraction at 290 K and 1 atm, and $I_{\text{sp,BG50\%\&Air50\%}}$ and $I_{\text{sp,BG70\%\&Air30\%}}$ are the calculated specific impulses by the partial-fill model of Endo et al. Figure 22 shows the estimated suctioned air fill fraction $ff_{\text{air,est}}$. From this figure, in the present experiment, we see that $0.175 \leq ff_{\text{air,est}} \leq 0.327$. It is confirmed that air, having almost the same volume order, is suctioned in the region $ff_{\text{propellant}} \geq 0.1$. It can be concluded that the multicycle PDRE has a partial-fill effect and that this effect may be mainly due to the suction air, which is consistent with the single-cycle partial-fill model of Endo et al.

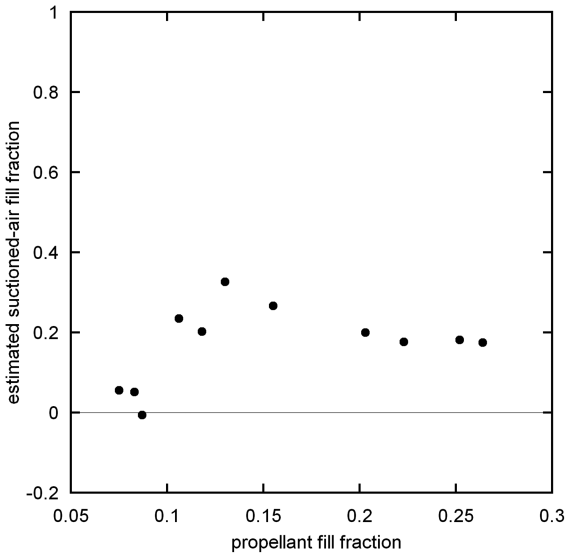

Fig. 22 Estimated volume fraction of air.

If the operation frequency becomes too high, the suctioned air volume may be small because exhaust time duration becomes small. In such a condition, the partial-fill effect may be very small. Contrastively, we believe we will be able to obtain a larger impulse from the ejector or other devices that can make use of the inertia of the air around the PDE tube more effectively.

IV. Conclusions

Multicycle PDE operation was achieved. In the thrust measurements using a load cell, the PDE's pulsed thrust was successfully smoothed and measured by a spring-damper-mass mechanism. The mass flow rate obtained by the direct cylinder mass difference measurement method was almost identical with that obtained by the cylinder pressure difference measurement method. As experimental results, specific impulses increased when the fill fraction was decreased. When the propellant partial-fill fraction was 0.130 ± 0.004, the specific impulse achieved a maximum value of 305 ± 9 s. The specific impulse sharply decreased as the fill fraction decreased below 0.130. This sharp decrease is considered to be due to the propellant gas densities becoming too small by diffusion and the propellant gas fill length becoming too short to initiate detonation waves in the PDE tube. Our calculations show that the multicycle PDRE has a partial-fill effect and that this effect may be mainly due to the suction air, which is consistent with the single-cycle partial-fill model of Endo et al. [21].

Acknowledgments

This research was supported by Hokkaido Technology Licensing Office Company, Ltd. This work was subsidized by the Regional Research and Development Consortium Project from the Hokkaido Bureau of Economy, Trade, and Industry; the Ministry of Education, Culture, Sports, Science, and Technology, a Grant-In-Aid for Young Scientists (B), No. 17760633; and the Industrial Technology Research Grant Program (2003 to 2006) from the New Energy and Industrial Technology Development Organization, No. 00B60027d and 03B64008c. The additional shadow-graph optical experiments were done by S. Shimada and K. Kawane of the University of Tsukuba.

References

[1] Nicholls, J. A., Wilkinson, H. R., and Morrison, R. B., "Intermittent Detonation as a Thrust-Producing Mechanism," *Jet Propulsion*, Vol. 27, No. 5, 1957, pp. 534–541.

[2] Bussing, T. R. A., and Pappas, G., "Pulse Detonation Engine Theory and Concepts," *Developments in High-Speed-Vehicle Propulsion Systems: Progress in Astronautics and Aeronautics*, Vol. 165, AIAA, Reston, VA, 1996, pp. 421–472.

[3] Kailasanath, K., "Review of Propulsion Applications of Detonation Waves," *AIAA Journal*, Vol. 38, No. 9, 2000, pp. 1698–1708. doi:10.2514/2.1156

[4] Kailasanath, K., "Recent Developments in the Research on Pulse Detonation Engines," *AIAA Journal*, Vol. 41, No. 2, 2003, pp. 145–159. doi:10.2514/2.1933

[5] Bazhenova, T. V., and Golub, V. V., "Use of Gas Detonation in a Controlled Frequency Mode (Review)," *Combustion, Explosion, and Shock Waves*, Vol. 39, No. 4, 2003, pp. 365–381. doi:10.1023/A:1024704602865

[6] Roy, G. D., Frolov, S. M., Borisov, A. A., and Netzer, D. W., "Pulse Detonation Propulsion: Challenges, Current Status, and Future Perspective," *Progress in Energy and Combustion Science*, Vol. 30, No. 6, 2004, pp. 545–672. doi:10.1016/j.pecs.2004.05.001

[7] Zitoun, R., and Desbordes, D., "Propulsive Performance of Pulsed Detonations," *Combustion, Science, and Technology*, Vol. 144, No. 1, Sept. 1999, pp. 93–114. doi:10.1080/00102209908924199

[8] Morris, C. I., "Numerical Modeling of Single-Pulse Gasdynamics and Performance of Pulse Detonation Rocket Engines," *Journal of Propulsion and Power*, Vol. 21, No. 3, 2005, pp. 527–538. doi:10.2514/1.7875

[9] Endo, T., and Fujiwara, T., "A Simplified Analysis on a Pulse Detonation Engine Model," *Transactions of the Japan Society for Aeronautical and Space Sciences*, Vol. 44, No. 146, 2002, pp. 217–222. doi:10.2322/tjsass.44.217

[10] Endo, T., Kasahara, J., Matsuo, A., Inaba, K., Sato, S., and Fujiwara, T., "Pressure History at the Thrust Wall of a Simplified Pulse Detonation Engine," *AIAA Journal*, Vol. 42, No. 9, 2004, pp. 1921–1929. doi:10.2514/1.976

[11] Wintenberger, E., Austin, J. M., Cooper, M., Jackson, S., and Shepherd, J. E., "Analytical Model for the Impulse of Single-Cycle Pulse Detonation Tube," *Journal of Propulsion and Power*, Vol. 19, No. 1, 2003, pp. 22–38. doi:10.2514/2.6099

[12] Cooper, M., Jackson, S., Austin, J., Wintenberger, E., and Shepherd, J. E., "Direct Experimental Impulse Measurements for Detonations and Deflagrations," *Journal of Propulsion and Power*, Vol. 18, No. 5, 2002, pp. 1033–1041. doi:10.2514/2.6052

[13] Talley, D. G., and Coy, E. B., "Constant Volume Limit of Pulsed Propulsion for a Constant γ Ideal Gas," *Journal of Propulsion and Power*, Vol. 18, No. 2, 2002, pp. 400–406. doi:10.2514/2.5948

[14] Wintenberger, E., and Shepherd, J. E., "Model for the Performance of Airbreathing Pulse-Detonation Engine," *Journal of Propulsion and Power*, Vol. 22, No. 3, 2006, pp. 593–603. doi:10.2514/1.5792

[15] Harris, P. G., Stowe, R. A., Ripley, R. C., and Guzik, S. M., "Pulse Detonation Engine as a Ramjet Replacement," *Journal of Propulsion and Power*, Vol. 22, No. 2, 2006, pp. 462–473. doi:10.2514/1.15414

[16] Ma, F., Choi, J.-Y., and Yang, V., "Propulsive Performance of Airbreathing Pulse Detonation Engines," *Journal of Propulsion and Power*, Vol. 22, No. 6, 2006, pp. 1188–1203. doi:10.2514/1.21755

[17] Kojima, T., and Kobayashi, H., "Thrust Increase of Air Breathing Pulse Detonation Engine by High Supply Pressure," *Space Technology Japan*, Vol. 4, 2005, pp. 35–42. doi:10.2322/stj.4.35

[18] Sato, S., Matsuo, A., Endo, T., and Kasahara, J., "Numerical Studies on Specific Impulse of Partially Filled Pulse Detonation Rocket Engines," *Journal of Propulsion and Power*, Vol. 22, No. 1, 2006, pp. 64–69. doi:10.2514/1.9514

[19] Wilson, J., Sgondea, A., Paxson, D. E., and Rosenthal, B. N., "Parametric Investigation of Thrust Augmentation by Ejectors on a Pulsed Detonation Tube," *Journal of Propulsion and Power*, Vol. 23, No. 1, 2007, pp. 108–115. doi:10.2514/1.19670

[20] Wilson, J., "Effect on Pulse Length and Ejector Radius on Unsteady Ejector Performance," *Journal of Propulsion and Power*, Vol. 23, No. 2, 2007, pp. 345–352. doi:10.2514/1.19665

[21] Endo, T., Yatsufusa, T., Taki, S., Matsuo, A., Inaba, K., and Kasahara, J., "Homogeneous-Dilution Model of Partially-Fueled Simplified Pulse Detonation Engines," *Journal of Propulsion and Power*, Vol. 23, No. 5, 2007, pp. 1033–1041. doi:10.2514/1.21223

[22] Zhdan, S. A., Mitrofanov, V. V., and Sychev, A. I., "Reactive Impulse from the Explosion of a Gas Mixture in a Semiinfinite Space," *Combustion, Explosion, and Shock Waves*, Vol. 30, No. 5, 1994, pp. 657–663. doi:10.1007/BF00755833

[23] Kasahara, J., Liang, Z., Browne, S. T., and Shepherd, J. E., "Impulse Generation by an Open Shock Tube," *AIAA Journal*, Vol. 46, No. 7, July 2008, pp. 1593–1603. doi:10.2514/1.27467

[24] Cooper, M. A., "Impulse Generation by Detonation Tubes," Ph.D. Thesis, California Inst. of Technology, Pasadena, CA, May 2004.

[25] Cooper, M., Shepherd, J. E., and Schauer, F., "Impulse Correlation for Partially Filled Detonation Tubes," *Journal of Propulsion and Power*, Vol. 20, No. 5, 2004, pp. 947–950. doi:10.2514/1.4997

[26] Schauer, F., Stutrud, J., and Bradley, R., "Detonation Initiation Studies and Performance Results for Pulsed Detonation Engine," AIAA Paper 2001-1129, 2001.

[27] Hirano, M., "Study on a Partially-Filled Pulse Detonation Rocket Engine," M.S. Thesis, Univ. of Tsukuba, Tsukuba, Japan, March 2005.

[28] Hirano, M., Kasahara, J., Matsuo, A., Endo, T., and Murakami, M., "Thrust-Performance Test of Ethylene–Oxygen Single-Tube Pulse Detonation Rocket," *Proceedings of the Asian Joint Conference on Propulsion and Power*, 2004, pp. 255–260.

[29] Kasahara, J., Hirano, M., Matsuo, A., Sato, S., Endo, T., and Satori, S., "Flight Experiments Regarding Ethylene–Oxygen Single-Tube Pulse Detonation Rocket," AIAA Paper 2004-3918, July 2004.

[30] Kasahara, J., "Pulse Detonation Rockets and Thrust Augmentation According to Partially-Filling Effect," *Journal of the Combustion Society of Japan*, Vol. 47, No. 140, 2005, pp. 84–89.

[31] Kasahara, J., Hasegawa, A., Nemoto, T., Yamaguchi, H., Yajima, T., and Kojima, T., "Performance Validation of a Single-Tube Pulse Detonation Rocket System," *Journal of Propulsion and Power*, Vol. 25, No. 1, 2009, pp. 173–180. doi:10.2514/1.37924

[32] Sakurai, T., Ooko, A., Yoshihashi, T., Obara, T., and Ohyagi, S., "Investigation of the Purge Process on the Multicycle Operations of a Pulse Detonation Engine," *Transactions of the Japan Society for Aeronautical and Space Sciences*, Vol. 48, No. 160, 2005, pp. 78–85. doi:10.2322/tjsass.48.78

[33] Reynolds, W. C., "The Element Potential Method for Chemical Equilibrium Analysis: Implementation in the Interactive Program STANJAN: Version 3," Stanford Univ., TR A-3991, Dept. of Mechanical Engineering, Stanford, CA, Jan. 1986.

J. Powers
Associate Editor